FLOW TRANSFORMATIONS IN PARTICULATE GRAVITY CURRENTS

DAVE WALTHAM
Department of Geology, Royal Holloway, University of London, Egham, Surrey TW20 0EX, U.K.
e-mail: d.waltham@gl.rhul.ac.uk

ABSTRACT: **The nature, thickness, and location of deposits from a particulate gravity current is strongly influenced by whether the flow is concentrated or dilute, whether it is laminar or turbulent, and whether it is supercritical or subcritical. These transitions are causally linked, because there is a clear contrast between a concentrated, laminar flow-type (e.g., pyroclastic flows and debris flows) and a dilute, turbulent flow-type (e.g., pyroclastic surges and turbidity currents). In this paper it is shown that the primary transition is from a dense to a less dense current, leading, in turn, to a transition from laminar to turbulent flow. This density transition can be caused by interface instability or by vigorous entrainment of ambient fluid at a hydraulic jump. It is also shown in this paper that hydraulic jumps occur at Froude numbers significantly different from unity. These concepts are confirmed by previously published data from a gravity current in the San Dimas Reservoir.**

INTRODUCTION

Gravity currents, in which a dense fluid underflows a less dense one, are widespread in the natural world (e.g., rivers and cold fronts; Simpson 1997). In particulate gravity currents the dense fluid is formed by particles suspended in a gas or liquid (e.g., an avalanche in which the dense fluid is a mixture of snow and air). Two types of particulate gravity current are of particular interest to sedimentologists. Explosive volcanic events give rise to pyroclastic surges and pyroclastic flows, in which the dense fluid is a mixture of hot gases, dust, and larger volcaniclastic fragments. In subaqueous environments, on the other hand, slope failure events can give rise to debris flows and turbidity currents, in which the dense fluid is a mixture of water, mud, sand, and larger siliciclastic fragments. For both environments there is a clear contrast between a concentrated, laminar flow-type (pyroclastic flows and debris flows) and a more dilute and turbulent flow-type (pyroclastic surges and turbidity currents). This immediately suggests that there is some causal link between the transition from a concentrated to a dilute flow and the transition from a laminar flow to a turbulent flow. However, the direction of the causal link is not obvious. A transition to turbulence might result in increased entrainment of ambient fluid, leading, in turn, to a rapid transition to a dilute flow. On the other hand it would seem equally plausible that a drop in flow density results in a drop in flow viscosity, leading to a transition to turbulence. This paper is concerned with sorting out these questions of cause and effect. These transitions are of much more than purely theoretical interest. The nature of the flow deposits, as well as their location and thickness, are strongly affected by these changes in flow properties.

Fisher (1983) specifically concentrated on the laminar-to-turbulent transition and identified four distinct routes for producing this transformation:

1. Body transformations, in which a flow changes from laminar to turbulent flow without significant change in density;
2. Gravity transformations, in which a flow segregates, by gravitational settling, into an underlying dense laminar flow and an upper dilute turbulent flow;
3. Surface transformations, in which ambient fluid becomes entrained in the upper part of the flow, leading, again, to an underlying dense laminar flow and an upper dilute turbulent flow;
4. Fluidization transformations, in which particles and fluids diffuse upwards from a dense laminar flow to produce an overlying dilute turbulent flow.

Body transformations imply that the laminar-to-turbulent transition occurs first and that this is followed by increased fluid entrainment and a transition to a low-density or density-stratified flow. The other three transformations are examples in which the primary transition is to a flow with density stratification. The low-density parts of that flow then subsequently become turbulent.

In addition to the high-density to low-density transition and the laminar-to-turbulent transition, there is a third important form of flow transition: the transition from a supercritical flow, in which flow is faster than the speed of a wave propagating across the flow surface, to a subcritical flow. This transition is important partly because supercritical and subcritical flows have very different characteristics. More importantly, however, the supercritical-to-subcritical transition is abrupt and leads to a very sharp change in flow speed and thickness known as a hydraulic jump. It is very plausible that an increase in turbulence, and/or the potential for flow stratification, might be associated with the changes at a hydraulic jump, and so this third flow transition type is also investigated in this paper.

In principle, these three transitions are distinct. For example, it is theoretically quite possible to have a transition from a laminar, high-density flow to a laminar, low-density flow. Nevertheless, several authors (e.g., Komar 1971; Hand 1974) have suggested that these transitions should be causally linked by, for example, enhanced fluid entrainment (high-density to low-density transition) at a hydraulic jump (supercritical to subcritical transition). Observations of real flows have been interpreted as supporting this conclusion (e.g., Weirich 1989; Piper et al. 1999).

This paper investigates these transitions using depth-averaged Equations closely related to those used by Chu et al. (1979) and Parker et al. (1986).

LAMINAR-TO-TURBULENT FLOW TRANSITIONS

The transition from a laminar to a turbulent flow is commonly investigated by calculating the Reynolds number

$$\mathrm{Re} = Dv\rho/\mu \tag{1}$$

where D is a typical flow dimension, v a typical velocity, ρ is density and μ is viscosity. This number expresses the relative sizes of inertial and viscous forces. Turbulence requires inertial forces large enough to overcome the tendency of viscosity to keep the flow well ordered. Hence, transition to turbulence occurs when the Reynolds number exceeds a critical value. For simple Newtonian fluids this critical value is approximately 10^3, but for more complex rheologies the critical value can be very much higher (Hampton 1972).

Taking the flow depth, h, as the appropriate typical dimension, and the depth-averaged flow velocity, $\bar{u}$, as the appropriate typical velocity, Equation 1 becomes

$$\mathrm{Re} = h\bar{u}\rho/\mu. \tag{2}$$

It is convenient to express this in terms of the mass flux, Q, of the flow given by

$$Q = h\bar{u}\rho W \tag{3}$$

where W is the mean flow width. Combining Equations 2 and 3 gives

$$\mathrm{Re} = Q/W\mu. \tag{4}$$

JOURNAL OF SEDIMENTARY RESEARCH, VOL. 74, NO. 1, JANUARY, 2004, P. 129–134
 1527-1404/04/074-129/$03.00

Hence, a transition from a laminar to a turbulent flow requires an increase in flux, a decrease in flow width, a fall in viscosity, and/or a drop in the critical value of the Reynolds number. Note that, in most flows, width increases with distance and the flow should tend to become less turbulent as it travels away from its source. In particular, Equation 4 shows that a body transformation (Fisher 1983) can occur only if the channel narrows. A body transformation will certainly not be induced by a simple increase in flow velocity (e.g., due to an increase in slope) because the effect of this is canceled by a corresponding decrease in flow thickness.

HIGH-DENSITY TO LOW-DENSITY TRANSITIONS

Despite the conclusions of the previous section, transitions from laminar to turbulent flow are commonly seen in nature. If this transition is not caused by a narrowing channel, Equation 4 implies that it is due to a decrease in viscosity and/or a decrease in the critical value of Reynolds number. These will both be affected by changes in flow density because at high suspended particle concentrations a fluid has a significantly increased viscosity and a finite yield strength. This inherent strength has the effect of suppressing turbulence, and the critical Reynolds number is therefore significantly higher than for a simple Newtonian fluid.

The simplest rheological model for a flow having a nonzero yield strength is a Bingham plastic (Hampton 1972), in which the basal shear stress is given by

$$\tau = K + \mu\left(\frac{\partial u}{\partial z}\right)_{z=0} = K + \mu F_0 \frac{\bar{u}}{h} = \frac{\mu \bar{u}}{h}(F_0 + B) \qquad (5)$$

where K is the yield strength of the fluid, z is the vertical coordinate measured upwards from the flow base, and B is the Bingham number, defined by

$$B = Kh/\mu\bar{u} \qquad (6)$$

F_0, in Equation 5, is a flow-profile parameter whose precise value depends upon the exact manner in which the flow velocity varies with height. A flow in which the velocity increases uniformly with height would have a gradient given simply by $\partial u/\partial z = 2\bar{u}/h$ (i.e., $F_0 = 2$) because the velocity would go from zero at the flow base to $2\bar{u}$ at the flow top. Other flow profiles (e.g., parabolic or logarithmic) have a different value of F_0.

Note that if the yield strength becomes negligible (i.e., $B << 1$) then Equation 5 reduces to that for a simple Newtonian fluid and the critical Reynolds number should be around 10^3. However, if the yield strength is significant, turbulence is suppressed and the critical Reynolds number is greatly increased. Hampton (1972) showed experimentally that the transition to turbulent flow occurs at a Reynolds number of approximately $1000B$. In the subsequent analyses, the critical Reynolds number is assumed to be the larger of 1000 or $1000B$. Note that the yield strength is strongly dependent upon the concentration of suspended particles and so, via Equation 6, the critical Reynolds number falls dramatically as flow density drops.

Many processes have been proposed for causing a density transition and these are neatly summarized by the gravity, surface, and fluidization transformations (Fisher 1983) discussed in the introduction.

Gravity transformations, i.e., gravitational settling as the flow slows (Lowe 1982), is important once the transition to turbulence has occurred. In turbulent flows suspension occurs only if the shearing velocity is significant compared with the particle fall velocity (Bagnold 1956), and suspension is therefore strongly dependent upon grain size and flow speed. In laminar flows, on the other hand, suspension results from the inherent strength of the fluid, and no settling occurs as a flow slows. It is therefore not possible to use a gravity transformation to explain the high-density to low-density transition given that this must occur before the laminar-to-turbulent transition.

The most common models of high-density to low-density transition are surface transformations caused by interface instability (Parker et al. 1986; Alexander and Morris 1994; Allen 1997), turbulence (Keulegan 1949), energetic mixing at a hydraulic jump (Komar 1971; Weirich 1989), or mixing at the flow head (Allen 1971; Hampton 1972).

Interface instability is controlled by the Richardson number, which expresses the size of the velocity gradient across the boundary relative to the density gradient across the boundary. It can be expressed in different ways depending upon the exact problem under investigation but for a constant density current the simplest form (see e.g., Alexander and Morris 1994 or Kneller et al. 1999) is

$$\mathrm{Ri} = g\Delta\rho h/\rho\bar{u}^2 = \mathrm{Fr}^{-2} \qquad (7)$$

where Fr is the Froude number defined by

$$\mathrm{Fr} = \bar{u}\sqrt{\rho/\Delta\rho g h} = \bar{u}/\sqrt{g' h} \qquad (8)$$

where g' is the reduced gravity and $\Delta\rho$ is the density contrast between the flow and the ambient fluid. Interface instability is expected whenever $\mathrm{Ri} < 0.25$ (i.e., $\mathrm{Fr} > 2$). Note that debris flows generally do not have a well defined density stratification, and so Equation 7 is a reasonable form of Richardson number to use. The conclusion that Froude number is an important control on surface instability is confirmed by Middleton's (1966) review of several studies, although he also concluded that the Reynolds number was important.

An alternative to interface stability is simple turbulent mixing across the flow–water interface. However, this is problematic because we require fluid entrainment first in order to get turbulence. Thus, for the particular problem investigated here of entrainment above a laminar flow, this mechanism is unlikely to be important.

Mixing at a hydraulic jump (Komar 1971; Weirich 1989) results from energetic secondary currents induced immediately after the jump (Bohr et al. 1996). These secondary currents are not turbulent because they have a very well defined structure and scale in both time and space. It should be emphasized that, from Equation 4, a jump cannot cause a transition to turbulence because there is no change in Reynolds number (the effect of increased thickness is canceled by the effect of reduced flow speed). Nevertheless, the secondary currents are extremely energetic and could easily be responsible for significant fluid entrainment. This possibility is investigated using the real debris-flow example mentioned above.

Allen (1971) and Hampton (1972) showed that the most efficient process for fluid entrainment was mixing at the flow head. In these papers, entrainment occurred as a result of shearing as the head moved under the almost stationary ambient fluid as well as by capture of ambient fluid in ''tunnels'' at the front of the head. This simple picture is not viable for the case of a steady state flow. However, the general concept of shearing at a low-density/high-density interface as a result of differential flow rates is still valid. One possible scenario is that a relatively thin low-density current, generated farther up the flow by interface instability, moves faster than the underlying dense current and hence produces shear. This hypothetical explanation clearly requires observational support and must therefore be considered to be rather speculative at present.

SUPERCRITICAL-TO-SUBCRITICAL TRANSITIONS

The final type of flow transition investigated in this paper is that from a supercritical to a subcritical flow. In a supercritical flow, the flow speed exceeds that for a wave traveling on the surface of the flow. If a small object is dropped into a subcritical flow, ripples spread out from the impact in all directions, whereas, if the same experiment is attempted in a supercritical flow, the ripples are swept downstream and no part of the flow upstream experiences any influence from the dropped object.

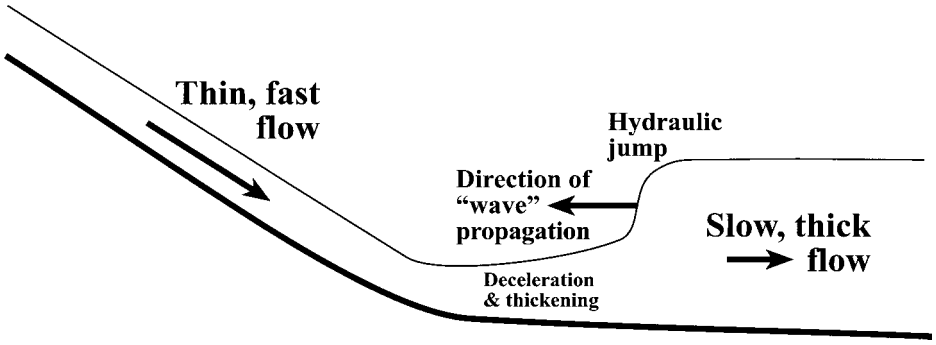

FIG 1.—A conceptual model for hydraulic jumps. At left the fast flow down the steeper slope is supercritical and thin. At right the horizontal slow flow is subcritical and thick. Hence, after the change in slope, the flow slows and thickens, giving rise to a nonhorizontal flow top. The flow tries to reestablish a horizontal upper surface by propagation of a wave from right to left. However, this wave cannot propagate beyond the point at which flow speed equals wave propagation speed, and hence a sharp jump occurs at this point.

This definition of criticality is all that is required to understand why flows, decelerating from supercritical to subcritical speeds, usually experience a sudden, dramatic increase in flow thickness at the critical point (i.e., a hydraulic jump). Figure 1 shows a steady-state gravity current moving supercritically down a slope and then decelerating, and therefore thickening, as it moves into a lower-slope region. Now, a flow consisting of a thicker part to the right is gravitationally unstable and so the thicker part tends to flow leftwards in the form of a wave. However, this wave is also carried rightwards by the underlying flow, and it is not able to propagate leftwards beyond the point where its wave propagation speed equals the flow speed. Hence, a jump in flow thickness occurs precisely at the point where these velocities are equal.

The important point about hydraulic jumps is that the flows not only thicken at the jump but also undergo a sudden, dramatic deceleration. The drop in velocity can result in a dramatic increase in sediment loss from the flow, which is important in its own right but can also indirectly influence the Reynolds number by changing the density, viscosity, and yield strength. However, as noted earlier, these changes happen only in a turbulent flow. Hydraulic jumps also occur in laminar flows (Craik et al. 1981; Bohr et al. 1993; Bohr et al. 1997; Rao and Arakeri 1998; Yokoi and Xiao 1999) and these have unaltered rheological properties after the jump unless the associated local instabilities and secondary currents (Craik et al. 1981; Bohr et al. 1997; Yokoi and Xiao 1999) result in greatly increased ambient fluid entrainment.

Hydraulic jumps occur when the Froude number reaches a critical value. Most studies assume that this critical value is unity (e.g., Komar 1971; Hand 1974). However, this is only approximately true as will be discussed below.

In a steady, uniform gravity flow, gravitational and frictional forces are in equilibrium, and so

$$\Delta\rho g h \tan\theta + \tau = 0 \tag{9}$$

where τ is the shear stress resulting from friction at the flow top and the flow base. In a steady but non-uniform flow, on the other hand, a more complex balance involving inertial forces is required. Appendix A shows that, for a two-dimensional flow with no density stratification,

$$\Delta\rho g h \tan\theta + \tau = \frac{\partial h}{\partial x}[\Delta\rho g h - \rho\overline{u}^2 F] \tag{10}$$

where

$$F = \frac{2}{\overline{u}^2}\left(\overline{u^2} + \overline{zu\frac{\partial u}{\partial z}}\right) - \frac{u(h)}{\overline{u}}. \tag{11}$$

The assumption that the current is not stratified is reasonable for a debris flow, as noted earlier, but may become poor for a turbidity current. Hence, the conclusions given below should be handled with care if applied to such cases.

Now, if the flow is not uniform, then from Equation 9 the left hand side of Equation 10 must be nonzero. This causes no mathematical difficulties except where

$$\Delta\rho g h \cong \rho\overline{u}^2 F \tag{12}$$

because $\partial h/\partial x$ must then become large. This is the hydraulic jump.

Comparing Equations 8 and 12 it can be seen that a hydraulic jump occurs when $\mathrm{Fr} = F^{-1/2}$. For a flow which has uniform velocity with depth Equation 11 reduces to $F = 1$, i.e., the standard result that hydraulic jumps are expected at a Froude number of 1. However, for depth-varying flows, F differs from unity.

THE SAN DIMAS RESERVOIR GRAVITY CURRENT

Subaerial Debris Flow

The San Dimas Reservoir debris flow (Weirich 1989) is a well documented data set for testing the preceding theory. There are quantitative data for the subaerial flow obtained from flumes placed in the flow path, and in addition the reservoir was drained, after the debris-flow events, enabling inspection of the resulting subaqueous deposits. For full details the interested reader is directed to the original paper.

For the purposes of this paper, the relevant data on the sub-aerial debris flow are that the gradient was 0.01, the flow density was 1500 kg m^{-3}, the flow thickness was 1 m and the flow top velocity was 6 m s^{-1}. It is also important to note that the largest clast in debris-flow deposits had a diameter of 5 cm and the clast density was 2500 kg m^{-3}. This information was taken directly from the text of Weirich (1989) except for the flow depth, which was estimated as follows. A photograph of the flume (Weirich 1989, fig. 2) shows a depth of about 1 m. Weirich (1989) also stated that, at their maximum, the flows just overtopped the flumes. Hence, the flow depths in the flumes were of the order of 1 m. This estimate can be confirmed by noting that, for the volume flux of 5 m^3 s^{-1} and a flow velocity around 5 m s^{-1}, the cross-sectional area of the flow should be 1 m^2. The V-shaped flume had a maximum width of about 2 m, and hence its cross-sectional area is, indeed, about 1 m^2.

The first property which can be deduced from these observations is the flow yield strength. The largest possible suspended clast diameter, $d_{\max}$, is related to the yield strength by (Raudkivi 1998):

$$d_{\max} = 6K/g\Delta\rho \tag{13}$$

which, for the observed 5 cm clasts, gives a yield strength of 82 Pa.

For a Bingham plastic flow the velocity profile is in the form of a parabolic increase from zero at the base to a maximum which occurs part way up the flow (Hampton 1972). Above this point there is a constant-velocity plug. For a subaerial flow the shear stress at the flow top is extremely small, and so the constant velocity plug should extend all the way to the flow surface. The thickness of this plug, h_p, can be calculated simply by noting that the gravitational shear stress at the plug base should equal the yield strength, i.e.

$$K = \Delta\rho g h_p \tan\theta. \quad (14)$$

This gives a plug thickness of 0.56 m. The assumption of a parabolic profile below this plug then implies, from Equation 5, that the viscosity is

$$\mu = \frac{K - \tau}{2u_{\max}}(h - h_p) \quad (15)$$

where the shear stress at the flow base, τ, is found from Equation 9. For this flow, Equation 15 gives a viscosity of 2.4 Pa s.

Now that the profile of velocity versus depth is constrained, the depth-averaged velocity can be found. For a flow with a parabolic lower section and constant-velocity upper plug, the average velocity is given by

$$\bar{u} = u_{\max}(1 - \beta/3) \quad (16)$$

where β is the ratio of parabolic thickness to total thickness, i.e., $\beta = (h - h_p)/h$. For the San Dimas flow $\beta = 0.44$ and hence the depth-averaged velocity is 5.1 m/s.

Equation 2 can now be used to estimate the Reynolds number as 3200. At first sight this suggests a turbulent flow. However, from Equation 6, the Bingham number was 6.7. Hence, the critical Reynolds number was approximately 6700 and the debris flow was laminar.

The fact that the flow was laminar and held material in suspension as a result of a nonzero yield strength, justifies the description of this as a debris flow even although its properties appear to be untypical of the majority of such flows (e.g., Sharp and Nobles 1953 give a maximum viscosity of 200 to 600 Pa s).

Finally, it is worth calculating the Froude number and critical Froude number for the subaerial flow. Using Equation 8, the flow Froude number was 1.6. Equation 11, for a flow of this form, becomes

$$F = \frac{2 - \frac{7}{15}\beta}{\left(1 - \frac{\beta}{3}\right)^2} - \frac{1}{1 - \frac{\beta}{3}}. \quad (17)$$

Hence, with $\beta = 0.44$, Equation 17 gives $F = 1.3$. The critical Froude number is therefore 0.88 and the flow was supercritical.

Subaqueous Debris Flow

The subaerial debris flow, discussed above, then plunged into a reservoir and could no longer be directly observed. However, on the basis of interpretation of the deposits, Weirich (1989) deduced that the subaqueous flow initially had a thickness of 0.5 m in a channel of width 5 m. Equation 3 therefore implies an average velocity around 2 m s^{-1}, and Equations 4 and 6 give a Reynolds number of 630 and a Froude number of 1.3. Note that the maximum possible critical Froude number given by Equation 17 is 1.0 (when $\beta = 0$). Hence, the flow remained laminar and supercritical.

However, these parameters could not be maintained, because the basal shear stress below a submerged, uniform flow 0.5 m thick is less than the yield strength. In other words, the drop in density contrast as the flow entered the water must have caused an eventual deceleration to well below the initial 2 m s^{-1}. The density contrast fell, on entering the water, by a factor of 3 (i.e., from 1500 kgm^{-3} to 500 kgm^{-3}) whilst the slope remained constant. Hence, the thickness of the constant-velocity plug given by Equation 14 will triple giving a minimum possible steady state flow thickness of 1.7 m. At this thickness, Equation 3 gives a flow velocity of 0.6 m s^{-1} and the Froude number falls to just 0.21. Note that these are upper estimates; in reality the flow thickened slightly beyond the minimum. Thus, the plunging of the flow into the reservoir gave the potential for a hydraulic jump, because the flow was initially supercritical but must eventually have become subcritical. Weirich's (1989) field observations indicate an abrupt thickening to 1.9 m after transport for around 130m and so the above analysis strongly supports his interpretation of this as a hydraulic jump.

Laminar–Turbulent Transition

The deeper-water deposits (Weirich's zones 3 and 4) show a transition from high-density debris-flow sediments to deposits more characteristic of low-density turbidity currents. Hence, there must have been entrainment of water, producing a low-density turbulent current riding above the debris flow.

As discussed earlier, this entrainment may have resulted from interface instability, and this possibility can be investigated using the Froude numbers calculated above. For the early subaqueous debris flow, Equation 7 indicates that interface instability was unlikely. It should be noted in addition that the yield strength of the debris flow significantly reduces surface instability and that deceleration of the flow reduces the Froude number further. Hence interface instability is unlikely to have been a significant factor causing fluid entrainment.

However, the high-density to low-density transition does seem to occur in the immediate aftermath of the hydraulic jump. This strongly suggests that there is significant mixing at the jump. It must be emphasized, however, that this is not the result of a transition to turbulence at the jump. The mixing is due to highly energetic secondary currents which have a well-defined, nonturbulent structure. This mixing, in turn, results in a drop in viscosity, an increase in flow volume, and a drop in the critical Reynolds number and so, via Equation 4, a transition to true turbulence can occur rapidly. This turbulence then magnifies the entrainment rate and so an abrupt transition to a low-density turbidity current occurs in the region after the jump.

CONCLUSIONS

This paper focuses on these types of transition in steady-state particulate gravity currents:

1. The transition from laminar flow to turbulent flow.
2. The transition from supercritical flow to subcritical flow at a hydraulic jump.
3. The transition from a high-density flow to a low-density flow.

These transitions are logically distinct but may well be causally connected, and it was the nature of such connections that was investigated here.

The first important conclusion is that Reynolds numbers are not affected by changes in flow thickness unless this is also accompanied by a change in channel width. In particular, the Reynolds number of a flow does not change as a direct result of a hydraulic jump. The increase in Reynolds number resulting from the increase in flow thickness is exactly canceled by a decrease in Reynolds number caused by a decrease in flow velocity across the jump. In fact, the Reynolds number of a flow generally drops with distance as a result of channel widening or lateral spreading of the flow beyond the channel exit.

Increase in the Reynolds number, and therefore transition to turbulence, can be achieved only by substantial entrainment of water into a flow. This has three effects:

1. The flow discharge increases.
2. The flow viscosity decreases.
3. The critical Reynolds number decreases.

All of these factors contribute to the transition to turbulence.

Hence, the most important process producing the laminar to turbulent transition is fluid entrainment, which also produces the high-density to low-density transition. These two transitions are therefore intimately linked. Unfortunately, the high-density to low-density transition is the least understood of the three transitions, with even the main mechanisms of fluid entrainment being in dispute.

Another important conclusion from this study is that the critical Froude number at which a hydraulic jump takes place is unity only for the special case of a flow which is uniform with depth. This conclusion is implicit in one or two earlier studies (e.g., Bohr et al. 1993) but does not seem to have been stated explicitly anywhere in the sedimentological literature. The critical Froude number is substantially below unity for the debris flow investigated in this paper.

The fact that critical Froude numbers are not unity for flows with non-uniform velocity versus depth is not surprising. From the earlier discussion it should be clear that hydraulic jumps occur when the surface wave velocity equals the flow speed, but for non-uniform flows, which flow speed should be used? It might be suspected, for example, that the important part of the flow in this context is the near surface where the wave occurs. In this case the important parameter would be the speed at the flow top. However, it is implicit, in the usual definition of Froude number, that the depth-averaged flow speed is the relevant quantity. In fact, the preceding detailed analysis shows that the relevant quantity is

$$\hat{u} = \bar{u}\sqrt{\mathrm{F}}. \tag{18}$$

Using this, it might be better to define a new profile-dependent Froude number which is indeed equal to unity at a hydraulic jump, i.e., redefine Fr as

$$\mathrm{Fr} = \hat{u}\sqrt{\rho/\Delta\rho g h} \tag{19}$$

Application of these ideas to the San Dimas Reservoir debris flow (Weirich 1989) gives results which are very compatible with Weirich's (1989) observations. In particular:

1. The subaerial flow had the properties required for a debris flow (i.e., a laminar flow with particle suspension due to a nonzero yield strength).
2. The subaqueous high-density flow underwent a hydraulic jump after about 100 m, giving an increase in thickness from 0.5 m to nearly 2 m. This jump occurred because the supercritical subaerial flow could not maintain its momentum in the subaqueous realm where the flow-driving density contrast was smaller.
3. Energetic secondary currents associated with the hydraulic jump probably produced a local increase in fluid entrainment. This, in turn, produced a drop in viscosity, an increase in total flux, and a drop in the critical Reynolds number. Hence, a transition to true turbulence was *indirectly* caused by the hydraulic jump.

The theory developed in this paper is based upon several assumptions. Most of the theory assumes steady-state flow, and therefore it cannot handle the important processes at the flow head. The theory also uses depth averaging, which restricts its application to situations in which the flow direction is not strongly dependent upon depth, although this is probably reasonable for most gravity flows. This depth averaging also results in expressions which might not be valid for a density-stratified flow. Use, for example, of Equation 11 to estimate critical Froude numbers in turbidity currents should be done with great care.

It is very clear from the work presented here that there is a pressing need for more experimental studies of fluid entrainment together with theoretical and numerical modeling of the possible processes responsible. In addition the prediction that depth-variable flows undergo hydraulic jumps at Froude numbers significantly less than unity needs to be tested.

ACKNOWLEDGMENTS

Thanks to Gary Nichols for reading the manuscript and making excellent suggestions for improvements. Thanks also to David Ulicny for his stimulating questions. Finally, thanks to Henry Pantin and Ben Kneller for insightful reviews which greatly enhanced this paper.

REFERENCES

Acheson, D.J., 1990, Elementary Fluid Dynamics: Oxford, U.K., Clarendon Press, 397 p.
Alexander, J., and Morris, S., 1994, Observations on experimental, nonchannelized, high-concentration turbidity currents and variations in deposits around obstacles: Journal of Sedimentary Research, v. A64, p. 899–909.
Allen, J.R.L., 1971, Mixing at turbidity current heads and its geological implications: Journal of Sedimentary Petrology, v. 41, p. 97–113.
Allen, P.A., 1997, Earth Surface Processes: Oxford, U.K., Blackwell Science, 404 p.
Bagnold, R.A., 1956, The flow of cohesionless grains in fluids: Royal Society, Philosophical Transactions, v. 249, p. 235–297.
Bohr, T., Dimon, P., and Putkaradze, V., 1993, Shallow water approach to the circular hydraulic jump: Journal of Fluid Mechanics, v. 254, p. 635–648.
Bohr, T., Ellegaard, C., Hansen, A.E., and Haaning, A., 1996, Hydraulic jumps, flow separation and wave breaking: an experimental study: Physica B, v. 228, p. 1–10.
Bohr, T., Putkaradze, V., and Watanabe S., 1997, Averaging theory for the structure of hydraulic jumps and separation in laminar free-surface flows: Physical Review Letters, v. 79, p. 1038–1041.
Chu, F.H., Pilkey, W.D., and Pilkey, O.H., 1979, An analytical study of turbidity current steady flow: Marine Geology, v. 33, p. 205–220.
Craik, A.D., Latham, R.C., Fawkes, M.J., and Gribbon, P.W., 1981, The circular hydraulic jump: Journal of Fluid Mechanics, v. 112, p. 347–362.
Fisher, R.V., 1983, Flow transformations in sediment gravity flows: Geology, v. 11, p. 273–274.
Hampton, M.A., 1972, The role of subaqueous debris flow in generating turbidity currents: Journal of Sedimentary Petrology, v. 42, p. 775–793.
Hand, B.M., 1974, Supercritical flow in density currents: Journal of Sedimentary Petrology, v. 44, p. 637–648.
Keulegan, G.H., 1949, Interface instability and mixing in stratified flows: National Bureau of Standards, Research Publication 2040.
Kneller, B.C., Bennett, S.J., and McCaffrey, W.D., 1999, Velocity structure, turbulence and fluid stresses in experimental gravity currents: Journal of Geophysical Research, v. 104, p. 5381–5391.
Komar, P.D., 1971, Hydraulic jumps in turbidity currents: Geological Society of America, Bulletin, v. 82, p. 1477–1488.
Lowe, D.R., 1982, Sediment gravity flows: II. Depositional models with special reference to the deposits of high-density turbidity currents: Journal of Sedimentary Petrology, v. 52, p. 279–297.
Middleton, G.V., 1966, Experiments on density and turbidity currents II. Uniform flow of density currents: Canadian Journal of Earth Sciences, v. 3, p. 627–637.
Parker, G., Fukushima, Y., and Pantin, H.M., 1986, Self-accelerating turbidity currents: Journal of Fluid Mechanics, v. 171, p. 145–181.
Piper, D.J.W., Cochonat, P., and Morrison, M.L., 1999, The sequence of events around the epicentre of the 1929 Grand Banks earthquake: initiation of debris flows and turbidity current inferred from sidescan sonar: Sedimentology, v. 46, p. 79–97.
Rao, A., and Arakeri, J.H., 1998, Integral analysis applied to radial film flows: International Journal of Heat and Mass Transfer, v. 41, p. 2757–2767.
Raudkivi, A.J., 1998, Loose Boundary Hydraulics: Rotterdam, A.A. Balkema, 496 p.
Sharp, R.P., and Nobles, L.H., 1953, Mudflow of 1941 at Wrightwood, Southern California: Geological Society of America, Bulletin, v. 64, p. 547–560.
Simpson, J.E., 1997, Gravity Currents: Cambridge, U.K., Cambridge University Press, 244 p.
Yokoi, K., and Xiao, F., 1999, A numerical study of the transition in the circular hydraulic jump: Physics Letters A, v. 257, p. 153–157.
Watanabe, S., Putkaradze, V., and Bohr, T., 2003, Integral methods for shallow free-surface flows with separation: Journal of Fluid Mechanics, v. 480, p. 233–265.
Weirich, F.H., 1989, The generation of turbidity currents by subaerial debris flows, California: Geological Society of America, Bulletin, v. 101, p. 278–291.

Received 31 January 2002; accepted 23 June 2003.

Appendix A: The Equation of Motion for a Two-Dimensional, Depth-Averaged Gravity Current

The general equation of motion for any continuous medium is given by the Cauchy Equation (see e.g., Acheson 1990)

$$\rho Du_i/Dt = \partial\tau_{ij}/\partial x_j + \rho g_i \tag{A1}$$

where u_i is a component of velocity, τ_{ij} a stress tensor component, x_j is a component of distance, and g_i a component of gravity. The indices i and j run over the x, y, and z directions, and z points vertically upwards with its origin at the flow base. The other fundamental Equation is the continuity equation, ensuring mass conservation:

$$\partial\rho/\partial t = -\nabla\cdot(\rho\mathbf{u}). \tag{A2}$$

Note that, for a Newtonian incompressible fluid, Equations A1 and A2 reduce to the Navier–Stokes Equations.

For a two-dimensional flow, assume that flow is in the x direction only, with all derivatives zero in the y direction. Also assume a steady state in which the flow characteristics at any given position do not change with time. Depth averaging the

x component of Equation A1, and making the assumption that the normal stresses equal the hydrostatic pressure, yields

$$-\frac{\partial P}{\partial x} + \frac{\tau}{h} = \rho\left[\overline{u\frac{\partial u}{\partial x}} + \overline{w\frac{\partial u}{\partial z}}\right] \tag{A3}$$

where P is the pressure, τ is the shear stress resulting from friction at the flow top and the flow base, w is the vertical velocity component and all quantities covered by a bar have been depth averaged. Note that the assumption of hydrostatic pressures is justifiable provided that the flow is thin (Watanabe et al. 2003).

The two-dimensional, steady state, constant density form of Equation A2 is

$$\partial u/\partial x + \partial w/\partial z = 0 \tag{A4}$$

which can be depth averaged, leading to

$$\partial \bar{u}/\partial x = w(h)/h \tag{A5}$$

where use has been made of the boundary condition $w(0) = 0$. The next step is to note that $w\partial u/\partial z = \partial/\partial z(uw) - u\partial w/\partial z$. Depth averaging this equation and combining the result with Equations A4 and A5 then yields

$$\overline{w\frac{\partial u}{\partial z}} = \overline{u\frac{\partial u}{\partial x}} - u(h)\frac{\partial \bar{u}}{\partial x}. \tag{A6}$$

Hence, Equation A3 becomes

$$-\frac{\partial P}{\partial x} + \frac{\tau}{h} = \rho\left[2\overline{u\frac{\partial u}{\partial x}} - u(h)\frac{\partial \bar{u}}{\partial x}\right]. \tag{A7}$$

At a hydraulic jump, there is a rapid change in flow thickness. Hence, to investigate the jump, all relevant terms in Equation A7 should be reexpressed in terms of the thickness gradient, $\partial h/\partial x$. The hydrostatic approximation allows the pressure gradient to be written explicitly in terms of flow geometry as

$$\frac{\partial P}{\partial x} = \Delta\rho g\frac{\partial H}{\partial x} = \Delta\rho g\left(\frac{\partial h}{\partial x} - \tan\theta\right) \tag{A8}$$

where H is the height of the flow top and θ is the slope of the underlying surface.

The term involving $\partial \bar{u}/\partial x$ can be modified by rewriting Equation A4 in the form $\partial/\partial x(h\bar{u}) = 0$. Hence,

$$\frac{\partial \bar{u}}{\partial x} = -\frac{\bar{u}}{h}\frac{\partial h}{\partial x}. \tag{A9}$$

Modification of the remaining term requires adoption of a similarity solution, i.e.,

$$u(z) = f(\alpha)\bar{u} \qquad \text{with } \alpha = z/h \text{ and } 0 < z < h. \tag{A10}$$

Hence it is assumed that the shape of the velocity profile, given by f, is a very slowly varying function of position. As a result, the derivatives of Equation A10 can be written as

$$\frac{\partial \bar{u}}{\partial x} = f\frac{\partial \bar{u}}{\partial x} - \frac{z\bar{u}}{h^2}\frac{\partial h}{\partial x}\frac{df}{d\alpha} \quad \text{and} \tag{A11}$$

$$\frac{\partial u}{\partial z} = \frac{\bar{u}}{h}\frac{df}{d\alpha}. \tag{A12}$$

Substituting Equations A9, A10 and A12 into A11 then yields

$$-\frac{\partial u}{\partial x} = \frac{u}{h}\frac{\partial h}{\partial x} + \frac{z}{h}\frac{\partial u}{\partial z}\frac{\partial h}{\partial x} \tag{A13}$$

and hence

$$\overline{u\partial u/\partial x} = (-[\overline{u^2} + \overline{zu\partial u/\partial z}]/h)\partial h/\partial x. \tag{A14}$$

Substitution of Equations A8, A9 and A14 into A7 then yields

$$\tau + \Delta\rho g h\tan\theta = \frac{\partial h}{\partial x}[\Delta\rho g h - \rho\bar{u}^2 F] \tag{A15}$$

where

$$F = \frac{2}{\bar{u}^2}\left(\overline{u^2} + \overline{zu\frac{\partial u}{\partial z}}\right) - \frac{u(h)}{\bar{u}}. \tag{A16}$$